

Article

Synthesis of Silica-Based Materials Using Bio-Residues through the Sol-Gel Technique

Karine Zanotti ¹, Katerine Igal ², María Belen Colombo Migliorero ², Vânia Gomes Zuin ^{1,3,4}
and Patricia Graciela Vázquez ^{2,*}

¹ Department of Chemistry, Federal University of São Carlos, São Carlos 13565-905, SP, Brazil; karinezanotti@hotmail.com (K.Z.); vaniaz@ufscar.br (V.G.Z.)

² Centro de Investigación y Desarrollo en Ciencias Aplicadas “Dr. Jorge J. Ronco” CINDECA, CONICET-CIC-UNLP, Facultad de Ciencias Exactas, Universidad Nacional de La Plata, La Plata 1900, Argentina; katerineigal@gmail.com (K.I.); mbmigliorero@quimica.unlp.edu.ar (M.B.C.M.)

³ Institute of Sustainable Chemistry, Leuphana University Lüneburg, 21335 Lüneburg, Germany

⁴ Green Chemistry Centre of Excellence, University of York, York YO10 5DD, UK

* Correspondence: pgvazquez@hotmail.com or vazquez@quimica.unlp.edu.ar; Tel.: +54-9-221-4288854

Abstract: This study focused on the use of citrus bio-waste and obtention of silica-based materials through the sol-gel technique for promoting a greener and more sustainable catalysis. The sol-gel method is a versatile synthesis route characterized by the low temperatures the materials are synthesized in, which allows the incorporation of organic components. This method is carried out by acid or alkali hydrolysis combined with bio-waste, such as orange and lemon peels, generated as co-products in the food processing industry. The main objective was to obtain silica-based materials from the precursor TEOS with different catalysts—acetic, citric and hydro-chloric acids and ammonium hydroxide—adding different percentages of lemon and orange peels in order to find the influence of bio-waste on acids/alkali precursor hydrolysis. This was to partially replace these catalysts for orange or lemon peels. The solids obtained were characterized with different techniques, such as SEM, FT-IR, potentiometric titration and XRD. SEM images were compared with pure silica obtained to contrast the morphology of the acidic and alkali hydrolysis. However, until now, few attempts have been made to highlight the renewability of reagents used in the synthesis or to incorporate bio-based catalytic processes on larger scales.

Keywords: sol-gel silica-based materials; acid/alkali hydrolysis; bio-waste; citrus peels



Citation: Zanotti, K.; Igal, K.; Colombo Migliorero, M.B.; Gomes Zuin, V.; Vázquez, P.G. Synthesis of Silica-Based Materials Using Bio-Residues through the Sol-Gel Technique. *Sustain. Chem.* **2021**, *2*, 670–685. <https://doi.org/10.3390/suschem2040037>

Academic Editors:

Francesca Deganello, Maria Luisa Testa and Sergio Gonzalez-Cortes

Received: 26 October 2021

Accepted: 23 November 2021

Published: 30 November 2021

Publisher's Note: MDPI stays neutral with regard to jurisdictional claims in published maps and institutional affiliations.



Copyright: © 2021 by the authors. Licensee MDPI, Basel, Switzerland. This article is an open access article distributed under the terms and conditions of the Creative Commons Attribution (CC BY) license (<https://creativecommons.org/licenses/by/4.0/>).

1. Introduction

Based on the main notions of the circular economy and the bioeconomy [1,2], the concept of using agricultural waste is discussed. The common objective is to minimize the generation of waste from economic or urban activities related to agriculture. The circular economy turns out to be attractive for understanding the sustainable challenges we face in terms of social, economic and environmental aspects. However, in the case of bio-waste, taking advantage of the immense amount of agricultural waste generated, the processes could become a complex and difficult operation [3]. This is especially true for the development of new materials from citrus fruit bio-waste.

Citrus fruits are believed to have originated from the warm southern slopes of the Himalayas in north-eastern India and northern Myanmar [4]. At present, citrus crops are among the most cultivated fruits in the tropical and subtropical regions of the world. Regarding the bio-waste issue, approximately one-third of citrus fruits are utilized for processing, which produces around 50–60% of organic waste [5].

With the growing importance that organic farming has acquired, both in developed and developing countries, there are no studies of these socio-economic realities [6]. Organic agriculture [7,8] has remained a haven against the invasion of agrochemicals and

industrialization in the food supply chain. It represents less than 1% of global agriculture, specifically reported as 0.98% by Willer and Lernoud [9]. On the contrary, agriculture is the fastest-growing food sector in the world [10]. South America has a strong presence in the agriculture sector: Argentina (3,191,255 ha), Uruguay (930,965 ha) and Brazil (705,233 ha) [9–11]. Approximately 40% of the oranges produced globally are used in the production of different commercial products [12]. Due to processing, large amounts of waste products (bio-waste), such as peels from the juice industry, are generated and accumulated [13].

Considering this waste accumulation, different investigations propose the use of waste and bio-waste in order to obtain new materials, especially in sol-gel synthesis to obtain silica-based materials [13–19]. The sol-gel process can be described as the formation of an oxidic network through the polycondensation reaction of a molecular precursor in a liquid. The term sol refers to a dispersion of colloidal particles in a liquid medium where the stability of the colloids is due to both Brownian motion and small particle size. The term gel refers to a three-dimensional network of a solid phase interwoven with an entrapped and immobilized continuous liquid phase [18–20]. In our previous research, the sol-gel method was used as a versatile synthesis route characterized by the low temperatures at which inorganic materials and organic/inorganic hybrids were synthesized [21,22].

In this research, two main issues were addressed at the same time: the use of citric bio-waste and the obtention of materials using the sol-gel technique—looking for their use in heterogeneous catalysis as a bi-functional support system. Silica has been identified as an ideal support material for its strong hydrophilicity, acknowledged biocompatibility, shape and chemistry surface [23]. Two different strategies have been explored to combine bio-waste with the synthesis of silica-based materials. The first step was to obtain silica through acidic or alkaline hydrolysis by using acetic, citric, hydrochloric acids and an alkali (ammonium hydroxide). In the second step, lemon or orange peels were added to the obtained mixtures. The objective of this mixed synthesis was to find the influence of organic bio-waste on acids/alkalis, to partially replace them with organic orange or lemon peels, which could presumably provide citric acid, among other compounds. For this, different amounts of bio-waste were used in the various syntheses [24,25].

As a precursor of silica, tetraethyl orthosilicate (TEOS) was used, and its hydrolysis and condensation were studied, using absolute ethanol as a green solvent due to its renewability [26,27]. This solvent plays an important role in the synthesis of silica-based materials, both in the case of the reaction with TEOS, once they act as a homogenizer agent for substances with different solubilities that participate in the condensation reaction, and with lemon and orange peels, extracting compounds of interest from them [28–30]. All synthesized solids were characterized in-depth by integrating different physical-chemical techniques, such as scanning electron microscopy (SEM) and x-ray diffraction (XRD). The chemical compositions of the solids were investigated through Fourier transform infrared spectroscopy (FT-IR) and the acidic properties by *n*-butylamine potentiometric titration.

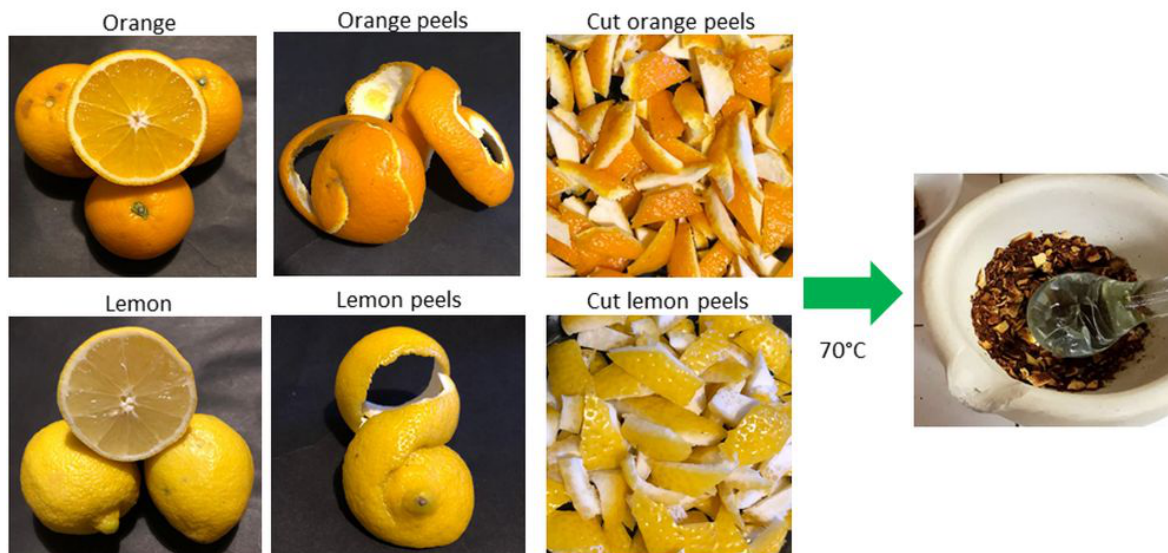
With the physicochemical properties discussed in this research, silica-based materials synthesized with bio-residues could have the potential to be used as supports for heterogeneous reactions (whose analysis is reserved for future research).

2. Materials and Methods

The starting point to specifying the proposed objectives includes having the necessary material and carrying out an adequate design of the experiments. For the design of these steps, two levels of complexity were selected, when required. This means that some of the operating variables remain fixed. Thus, reliable results can be obtained with the fewest possible experiences [21,22].

Before starting with the sol-gel synthesis, the oranges and lemons were peeled (20 of each of them), and the peels were cut into small pieces and put on the stove for 3 days, at 70 °C. Once calcined, the peels become brittle, and it is easier to grind them to a small size, so they were ground in a mortar (Scheme 1). This size allows uniformity between the

liquid gel and ground peels mixture. It should be noted that in 2020 a doctoral thesis was carried out with citrus peels without calcining (lemon, orange and mandarin) to obtain silica-based materials [31].



Scheme 1. Treatment of lemon and orange peels.

The sol-gel synthesis was carried out in a chamber with a nitrogen-controlled atmosphere at room temperature. First, a portion of the solvent, absolute ethanol ($\text{CH}_3\text{CH}_2\text{OH}$, Carlo Erba), and the corresponding catalyst for acid hydrolysis were placed into a beaker: acetic acid glacial (CH_3COOH , HPLC grade, J. T. Baker), citric acid ($\text{C}_6\text{H}_8\text{O}_7$ anhydrous for synthesis, Merck) or hydrochloric acid (HCl , 37%, Merck). The same was done in the alkaline hydrolysis using ammonium hydroxide (NH_4OH , Anedra analytical reagent). Then, the TEOS ($\text{Si}(\text{OC}_2\text{H}_5)_4$, Aldrich 98%) was added, followed by the last portion of solvent and distilled water, respectively.

Each mixture, outside the nitrogen-controlled atmosphere, was placed on a magnetic stirrer at 500 rpm; the respective amounts of orange or lemon peels were added, maintaining stirring for 2 h. The mixture was left for 3 weeks at room temperature; then, the gel formed was dried at $100\text{ }^\circ\text{C}$ for 1 h. The details of each synthesis are shown in Tables 1–4 (considering the total volume of ethanol added). Each table details the ratios of the compounds and the amounts used of lemon and orange peels (25 and 50%) in relation to the pure silica mass—considering as 100% the 5 g of pure silica obtained with fixed volumes of 17 mL of TEOS and 21.8 mL and, as appropriate, 5 mL of CH_3COOH ; 0.43 mL of $\text{C}_6\text{H}_8\text{O}_7$; 7.5 mL of HCl (so proton concentration is the same in all cases) or 1.8 mL of NH_4OH . The amounts of all the reagents were varied in order to maintain the relationship between the TEOS precursor, the acid and alkaline catalysts and the solvent, with which the same silica-based solids should be generated, but adding citrus peels.

The evaluation of the acidic properties was carried out by potentiometric titration with *n*-butylamine using a Metrohm 794 Basic Titrino titrator (Switzerland) with a double-junction electrode. For that, 0.025 mL/min of an *n*-butylamine solution in acetonitrile (0.025 N) was added to 0.025 g of sample, previously suspended in 45 mL of acetonitrile and keeping the stirring time constant (540 s) before adding the first drop and a waiting time of the drop of 60 s, while stirring constantly. FT-IR spectrum was obtained using Bruker IFS 66 equipment (Germany). Pellets of the sample in KBr, at room temperature, were measured in a range between 500 and 4000 cm^{-1} . SEM was applied to obtain different micrographs of the solids using the JEOL equipment, JSM-6390LV (Japan), with a voltage of 20 kV. Samples were supported on graphite and metalized with a sputtered gold film. Finally, XRD patterns were recorded by means of a PANalytical X'Pert Pro 3373/00 device

with the following conditions: Cu K α radiation ($\lambda = 1.5417 \text{ \AA}$); Ni filter; 20 mA and 40 kV in the high voltage source; scanning angle (2θ) from 5° to 40° , scanning rate $2^\circ (2\theta)/\text{min}$.

Table 1. Conditions employed in silica synthesis using acetic acid as a catalyst.

Sample	Precursor	Solvent	Acid	Water	Bio-Waste
KZ1	TEOS 17.0 mL	EtOH 21.8 mL	CH ₃ COOH 5.0 mL	H ₂ O 5.0 mL	Pure silica 5.0 g
KZ2	TEOS 8.5 ml	EtOH 10.9 mL	CH ₃ COOH 2.5 mL	H ₂ O 2.5 mL	50% orange peel 2.5 g
KZ3	TEOS 12.8 mL	EtOH 16.3 mL	CH ₃ COOH 3.75 mL	H ₂ O 3.75 mL	25% orange peel 1.25 g
KZ4	TEOS 8.5 mL	EtOH 10.9 mL	CH ₃ COOH 2.5 mL	H ₂ O 2.5 mL	50% lemon peel 2.5 g
KZ5	TEOS 12.8 mL	EtOH 16.3 mL	CH ₃ COOH 3.75 mL	H ₂ O 3.75 mL	25% lemon peel 1.25 g

Table 2. Conditions employed in silica synthesis using citric acid as a catalyst.

Sample	Precursor	Solvent	Acid	Water	Bio-Waste
KZ6	TEOS 17.0 mL	EtOH 21.8 mL	C ₆ H ₈ O ₇ 0.43 mL	H ₂ O 5.0 mL	Pure silica 5.0 g
KZ7	TEOS 8.5 ml	EtOH 10.9 mL	C ₆ H ₈ O ₇ 0.20 mL	H ₂ O 2.5 mL	50% orange peel 2.5 g
KZ8	TEOS 12.8 mL	EtOH 16.3 mL	C ₆ H ₈ O ₇ 0.30 mL	H ₂ O 3.75 mL	25% orange peel 1.25 g
KZ9	TEOS 8.5 mL	EtOH 10.9 mL	C ₆ H ₈ O ₇ 0.20 mL	H ₂ O 2.5 mL	50% lemon peel 2.5 g
KZ10	TEOS 12.8 mL	EtOH 16.3 mL	C ₆ H ₈ O ₇ 0.30 mL	H ₂ O 3.75 mL	25% lemon peel 1.25 g

Table 3. Conditions employed in silica synthesis using hydrochloric acid as a catalyst.

Sample	Precursor	Solvent	Acid	Water	Bio-Waste
KZ11	TEOS 17.0 mL	EtOH 21.8 ml	HCl 7.5 mL	H ₂ O 5.0 mL	Pure silica 5.0 g
KZ12	TEOS 8.5 ml	EtOH 10.9 mL	HCl 3.8 mL	H ₂ O 2.5 mL	50% orange peel 2.5 g
KZ13	TEOS 12.8 mL	EtOH 16.3 mL	HCl 5.6 mL	H ₂ O 3.75 mL	25% orange peel 1.25 g
KZ14	TEOS 8.5 mL	EtOH 10.9 mL	HCl 3.8 mL	H ₂ O 2.5 mL	50% lemon peel 2.5 g
KZ15	TEOS 12.8 mL	EtOH 16.3 mL	HCl 5.6 mL	H ₂ O 3.75 mL	25% lemon peel 1.25 g

Table 4. Conditions employed in silica synthesis using ammonium hydroxide as a catalyst.

Sample	Precursor	Solvent	Alkali	Water	Bio-Waste
KZ16	TEOS 17.0 mL	EtOH 21.8 ml	NH ₄ OH 11.8 mL	H ₂ O 5.0 mL	Pure silica 5.0 g
KZ17	TEOS 8.5 ml	EtOH 10.9 mL	NH ₄ OH 5.9 mL	H ₂ O 2.5 mL	50% orange peel 2.5 g
KZ18	TEOS 12.8 mL	EtOH 16.3 mL	NH ₄ OH 8.8 mL	H ₂ O 3.75 mL	25% orange peel 1.25 g
KZ19	TEOS 8.5 mL	EtOH 10.9 mL	NH ₄ OH 5.9 mL	H ₂ O 2.5 mL	50% lemon peel 2.5 g
KZ20	TEOS 12.8 mL	EtOH 16.3 mL	NH ₄ OH 8.8 mL	H ₂ O 3.75 mL	25% lemon peel 1.25 g

3. Results and Discussion

3.1. Digital Photographs

Among the basic principles of the sol-gel technique [32] is that it is an alternative to obtain non-metallic inorganic materials, such as glass and ceramics. This consists of the hydrolysis and condensation, originating from alkoxide precursors to form a polymeric network in the vitreous state, typically exhibiting a macroporous structure [33]. The gel is formed by a two-stage reaction: (1) hydrolysis and (2) polycondensation:

(1) The hydrolysis for gel formation is carried out using different alcohols as the solvent. This reaction is produced by the nucleophilic attack of the oxygen present in the water on the metal atom, forming silanols groups [34]. The solvent is the chemical compound that represents the largest proportion of the process.

(2) The condensation begins as soon as the alkoxide groups are hydrolyzed. The concentrations of -OH and/or -OR end groups depend on the hydrolysis and condensation mechanisms. They are determined by the nature of the catalyst used [35]. Brinker and Scherer [26] studied the effect of pH on the morphology of the siliceous structures. They found that the change in the pH of the solution affects the rates of hydrolysis and condensation, respectively. Figure 1 shows the silica synthesized with acid hydrolysis using acetic acid. The first photograph (pure silica) shows the silica obtained without bio-waste, with its glassy structure, coming from a gel that slowly dried at room temperature.

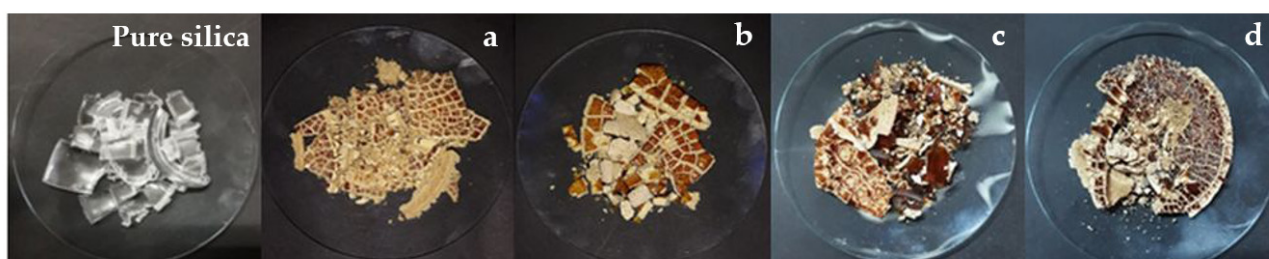


Figure 1. Silica gel obtained with CH₃COOH: (a) 50% orange peel; (b) 25% orange peel; (c) 50% lemon peel; (d) 25% lemon peel.

Milea et al. [36] found that the sol-gel technique allows the preparation of a new glass composition with superior properties determined by the specific properties of the gel [37,38]. In the following, Figure 1a,b correspond to the silica-based materials with orange peel aggregates, and Figure 1c,d correspond to silica-based materials with lemon peels. It is important to note that in all cases, the added peels remained in the siliceous structure, mainly on the surface of the dry gel, due to condensation; this occurred as the gel dried. If Figure 1a and c are compared, it can be distinguished that with 50% orange or lemon peel, the silica-based solid turns yellowish and has a surface structure similar

to pure silica. This layer of siliceous material is brighter and has a vitreous consistency. However, in the case of 25% orange and lemon peel added to the gel mixture, when drying, they are less shiny, although the surface is similar to 50% added bio-residues.

In the case of the 50% lemon or orange peel, the silica-based solid obtained forms two phases: one given by the compounds extracted by the solvents (ethanol and water) from the peels, varying the pH [25], and the other phase by the acid used in the synthesis. In the case of 25% peels, the effect is the same, although the pH is lower [28,39]. At this point, it is interesting to compare the gelation when the hydrolysis has already been carried out. Gelation is physically manifested by a drastic increase in the viscosity of the solution [40]. These changes in viscosity occur without causing the generation of chemical transformations or endothermic or exothermic changes [41]. The wet gel can be strengthened by aging and by the syneresis mechanism of Ostwald maturation [42]. The syneresis is characterized by the contraction of the gel network, produced by the expulsion or extraction of liquid. The gel that is a homogeneous substance becomes a segregation of solid components. Smaller particles have a higher solubility, which leads to their precipitation and the formation of larger ones [39]. During drying, the effect of citrus peels on the surface of the solids obtained indicates that the silicon skeleton becomes increasingly rigid. When the surface tension cannot deform the network, the gel body becomes too stiff. At this point, the likelihood of it breaking is higher [37,43], as can be seen in the photographs.

3.2. Potentiometric Titration Characterization

The acid properties of all the synthesized solids were studied through potentiometric titration with *n*-butylamine, which allows knowing the number of acid sites and their acid strength. To interpret the results obtained, the initial electrode potential (E_i) indicates the maximum acid strength of the surface sites, and the values of m eq/g solid, in which the plateau is reached, indicate the total number of acid sites. The acid strength of the surface sites can be classified according to the following ranges: very strong sites $E_i > 100$ mV, strong sites $0 < E_i < 100$ mV, weak sites $-100 < E_i < 0$ mV and very weak sites $E_i < -100$ mV, respectively. It is important to clarify that this technique only indicates the mass acidity trend of the solids obtained [44]. The initial electrode potentials are shown in Table 5 and their respective potentiometric curves in Figure 2.

Table 5. Initial electrode potential (E_i) values of the silica-based solid synthesized.

Sample	E_i (mV)	Sample	E_i (mV)
KZ1	128	KZ11	632
KZ2	110	KZ12	582
KZ3	132	KZ13	604
KZ4	89	KZ14	585
KZ5	117	KZ15	604
KZ6	275	KZ16	107
KZ7	72	KZ17	112
KZ8	104	KZ18	38
KZ9	118	KZ19	116
KZ10	187	KZ20	96

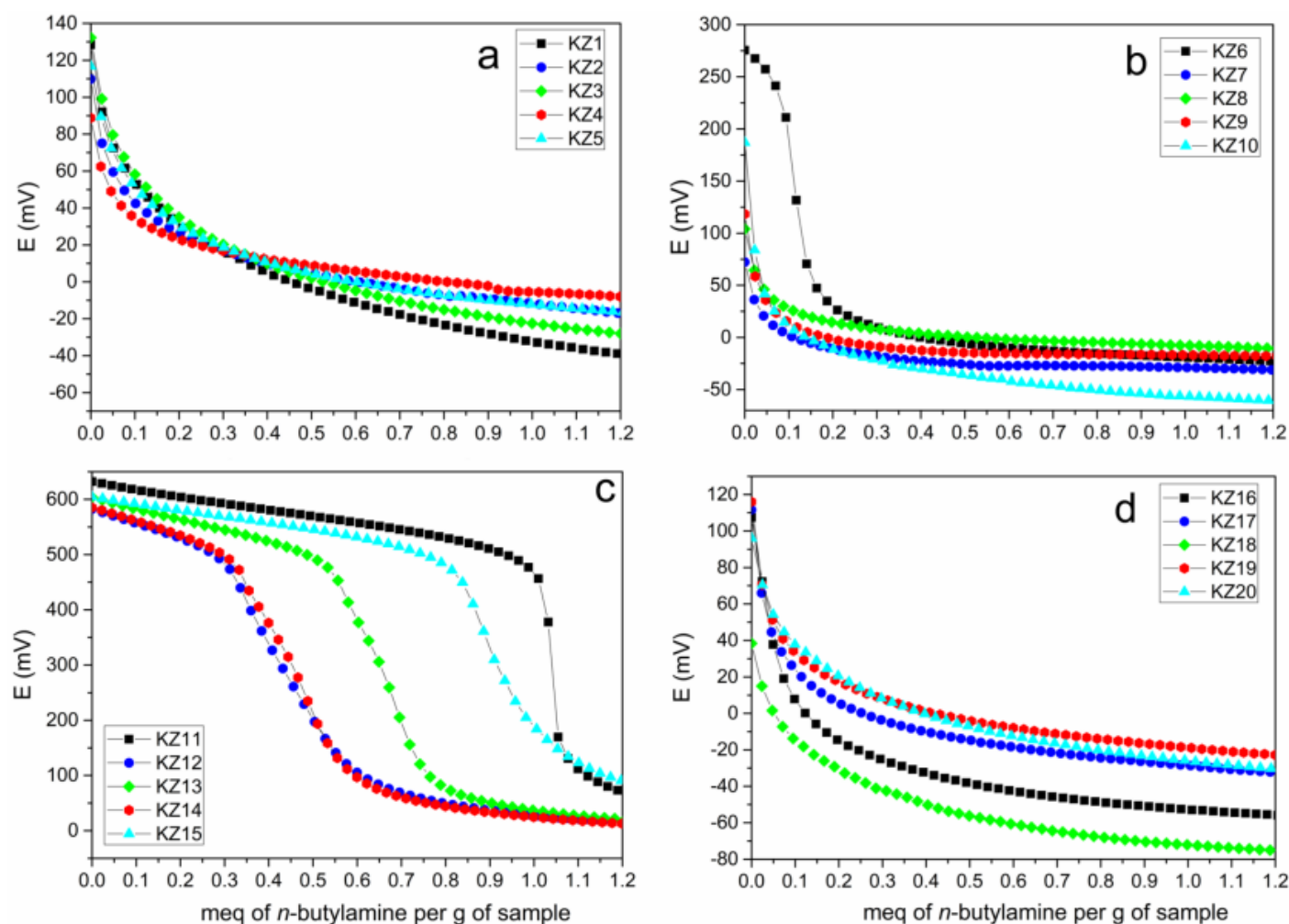


Figure 2. Potentiometric curves of the synthesized solids: (a) Acid hydrolysis: acetic acid (KZ1, KZ2, KZ3, KZ4, KZ5); (b) citric acid (KZ6, KZ7, KZ8, KZ9, KZ10); (c) hydrochloric acid (KZ11, KZ12, KZ13, KZ14, KZ15); (d) alkali hydrolysis: ammonium hydroxide (KZ16, KZ17, KZ18, KZ19, KZ20).

Comparing the potentiometric curves of the synthesis with acid hydrolysis (Figure 2a–c)—samples that use acetic, citric and hydrochloric acid—the presence of free electrons in the acid gave a higher acidity (Figure 2c). Comparing the use of 50 and 25% orange peels in acid hydrolysis versus pure silica (with acetic acid), KZ1 gives an E_i of 128 mV for pure silica versus 110 mV for 50% (KZ2) and 132 mV for 25% (KZ3) (Table 5). Citric and hydrochloric acid showed similar behavior to acetic acid when silica-based solid synthesized with orange and lemon peels were analyzed (Figure 2b,c). For basic hydrolysis, the use of NH_4OH generated the lowest value in both cases of 50 and 25% of the bio-waste. In the case of lemon peel, for both 50 and 25%, the E_i values (Table 5) and the potentiometric curves (Figure 2d) followed the same trend as those obtained for orange peels.

Among the constituents of lemon, approximately 70% correspond to citric acid, while folic and ascorbic acid are the predominant constituents in orange [31]. The incorporation of bio-waste in the structure of silica prepared by acid hydrolysis maintains the same E_i as the initial one, or decrease for all cases, since the acidity of the acids used as catalysts was greater than that of the bio-waste (compare E_i of Table 5 in the KZ11–Z13 series for orange and in the KZ11–KZ15 series for lemon). Although lemon was more effective in maintaining the high number of acidic sites for the samples synthesized with hydrochloric acid (compare the two series in Figure 2c), this trend did not hold for the samples synthesized with acetic or citric acid. Furthermore, at this point, one can see that none of the bio-residues contributed

new strong acid sites to the final material because the acidity of pure silica was “diluted” by the incorporation of orange or lemon peels.

When ammonium hydroxide was used, the acidic sites of the bio-waste were neutralized by the ammonia. Therefore, when the bio-waste amount was only 25%, the acidity of the bio-waste was neutralized and, hence, the obtained E_i of KZ18 (38 mV) and KZ20 (96 mV) was lower than pure silica KZ16 (107 mV). On the other hand, when the bio-waste amount was 50%, the acidity of the obtained silica slightly increased in comparison with the pure silica, as can be seen in the E_i values of KZ17 (112 mV) and KZ19 (116 mV), which can be understood as a contribution of the bio-residue to the final material acidity, slightly increasing it.

3.3. SEM Characterization

The pH of the catalyst determines the texture of the solid product, as can be seen in Figure 3. The morphology caused by acid hydrolysis (KZ1, KZ6 and KZ11) is laminar and typical of sol-gel silica. Curran and Stiegman [45] studied the morphology of siliceous structures at very high acidic concentrations; below the isoelectric point, dry xerogels become mesoporous. This is due to the protonation of silanols ($-\text{SiOH}$) to produce ($-\text{SiOH}_2^+$), which are leaving groups and increase the rate of condensation. First, hydrated monomers obtained from the hydrolysis of precursors undergo condensation reactions, forming silicate polymer chains and then small nuclei. These grow through silica monomer and polymer bonding, forming primary particles, usually 5–7 nm in mean diameter. Then, primary particles aggregate, producing larger SiO_2 particles that grow up to a stationary critical size [46]. In contrast, alkaline hydrolysis (KZ16) gives clusters of spheres because it is slower hydrolysis (formation of branched polymers or spherical aggregates). As expected, the use of only one alkoxide combined with appropriately chosen amounts of reagents allows for deep control over the nucleation and growth processes, leading to spherical and highly monodisperse nanoparticles [47].

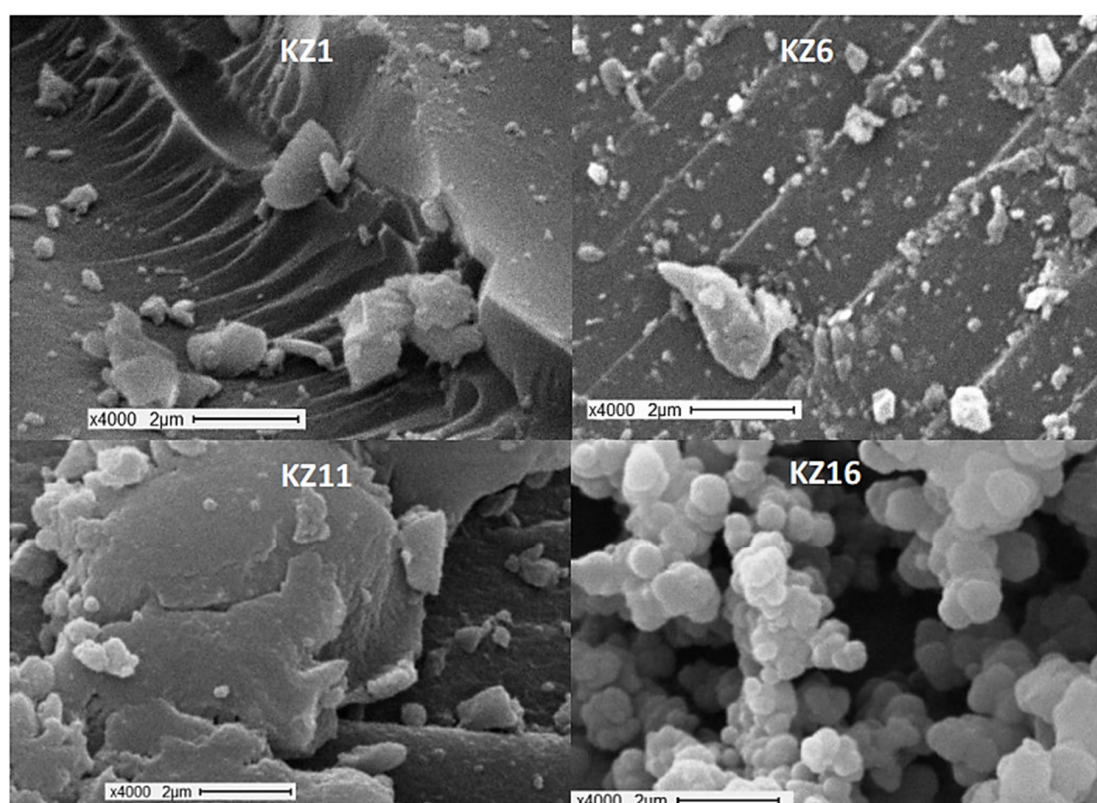


Figure 3. SEM micrographs of synthesized silica-based solid by acid (KZ1, KZ6 and KZ11) and alkali (KZ16) hydrolysis. Magnification $\times 4000$ (scale bar: 2 μm).

Regarding the SEM micrographs, Figure 4 shows the samples prepared with HCl as a catalyst. It was possible to observe a similarity to the characteristic laminar format of silica regardless of the amounts of orange or lemon that were added to the synthesis. In this case, hydrolysis with the strong acid can form, on the one hand, only silica and, on the other, leach the shells, as can be seen in the micrographs. Zarib and Abdullah [48] obtained a smooth surface and a rough surface together in the silicate particle. This was when rice husk was used as a bio-waste.

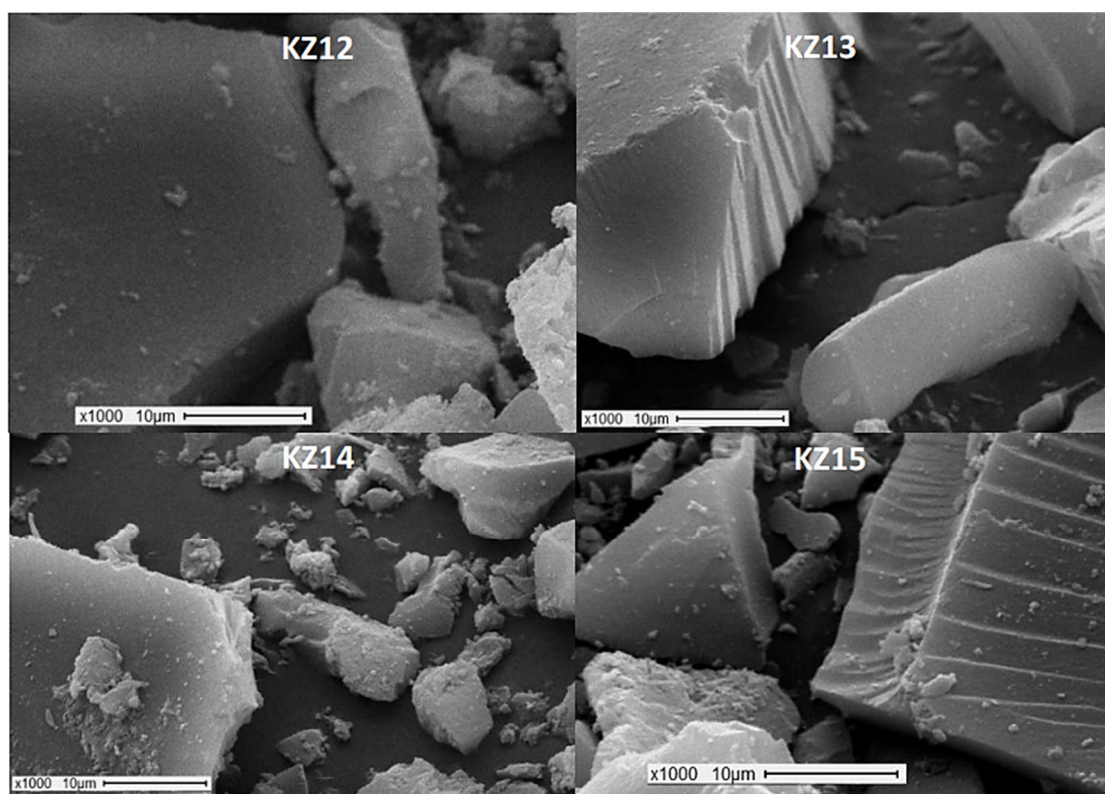


Figure 4. SEM micrographs of the silica-based solid synthesized using HCl with orange and lemon peels. Magnification $\times 1000$ (scale bar: 10 μm).

The NH_4OH sample, which can be seen in Figure 5, had a rounded shape and its particles formed clusters of variable sizes, which may be due to the action of orange and lemon aggregates that modify the pH of the synthesis. An agglomeration of nanoparticles of silica-based material and bio-waste was observed due to the three-dimensional hydrophilic networks on the surface of the solids [49]. Other researchers have synthesized silica with low surface microspheres from wheat husk ash with an alkaline and acid precipitation process [50].

3.4. XRD Characterization

The structure of the synthesized materials was determined using the XRD technique. This conventional technique has been increasingly used in similar studies for mixed matrices using bio-waste, such as the work developed by Worathanakul et al. [51] in which bagasse ash was used as a silica source for zeolite synthesis, another alternative source for the production of valuable materials and chemicals.

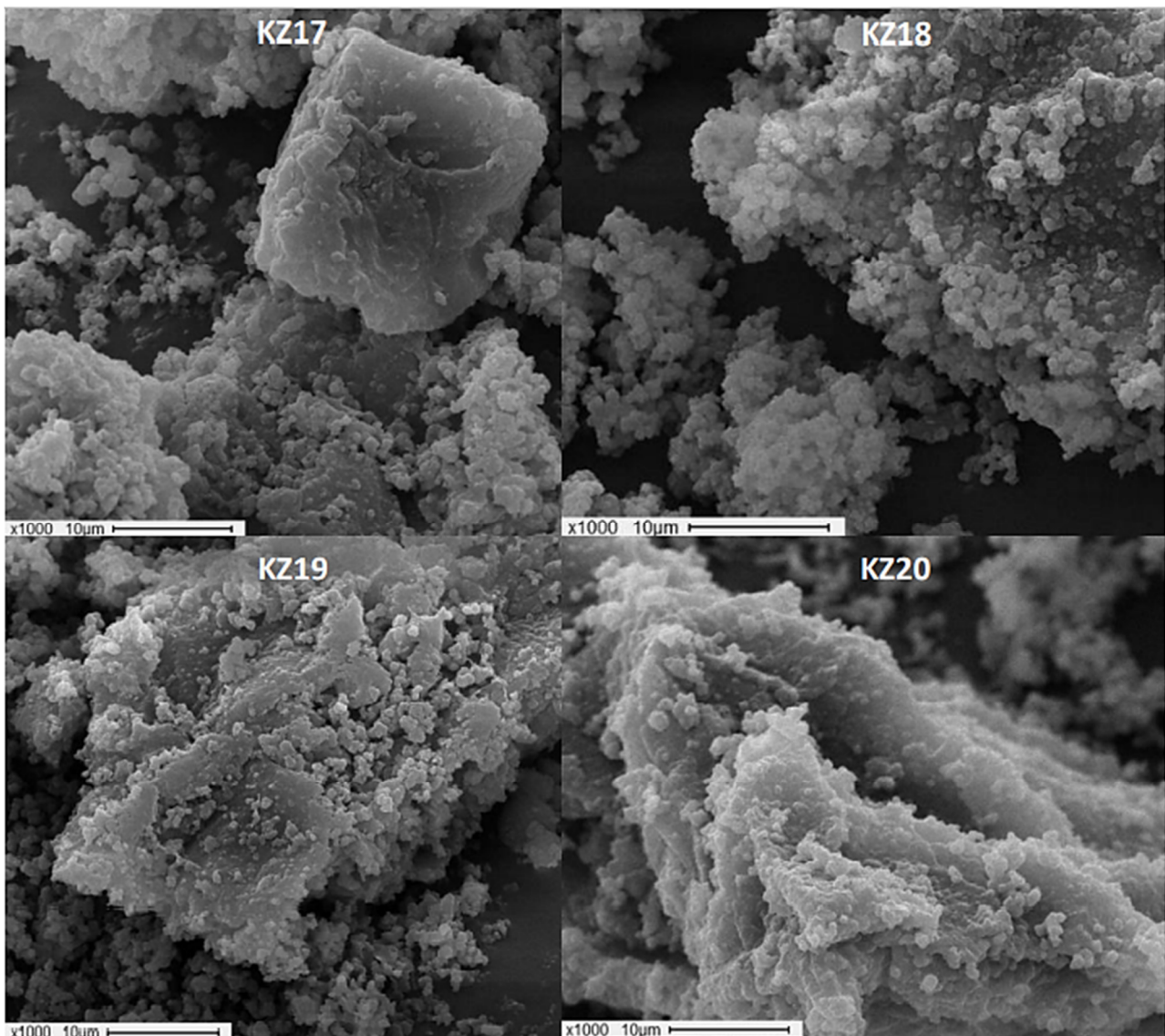


Figure 5. SEM micrographs of the silica-based solid synthesized using NH_4OH with orange and lemon peels. Magnification $\times 1000$ (scale bar: 10 μm).

Figure 6 shows the x-ray diffraction diagrams of the silica obtained using TEOS as a precursor employing the acids (acetic, citric and hydrochloric) and the alkali (ammonium hydroxide) as catalysts. The amorphous structure of silica xerogels was confirmed by the broad peaks in the interval around $15\text{--}30^\circ 2\theta$, as reported by Czarnobaj [52], and by the band located around $23^\circ 2\theta$, which is the typical diffraction of this type of silica [53,54].

Figure 7 presents the XRD diagrams of the synthesized silica-based solids with 50%, and 25% orange and lemon peels with acidic and alkali hydrolysis. The similarity of the diagrams with the silica without the addition of bio-waste indicates that the surface of the solids obtained was mostly silica-based solids.

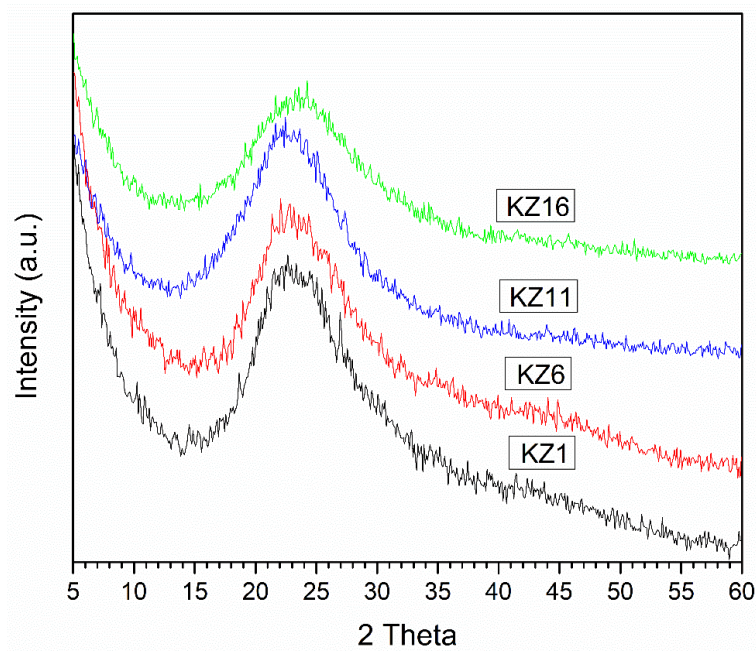


Figure 6. XRD diagram of silica-based solid synthesized.

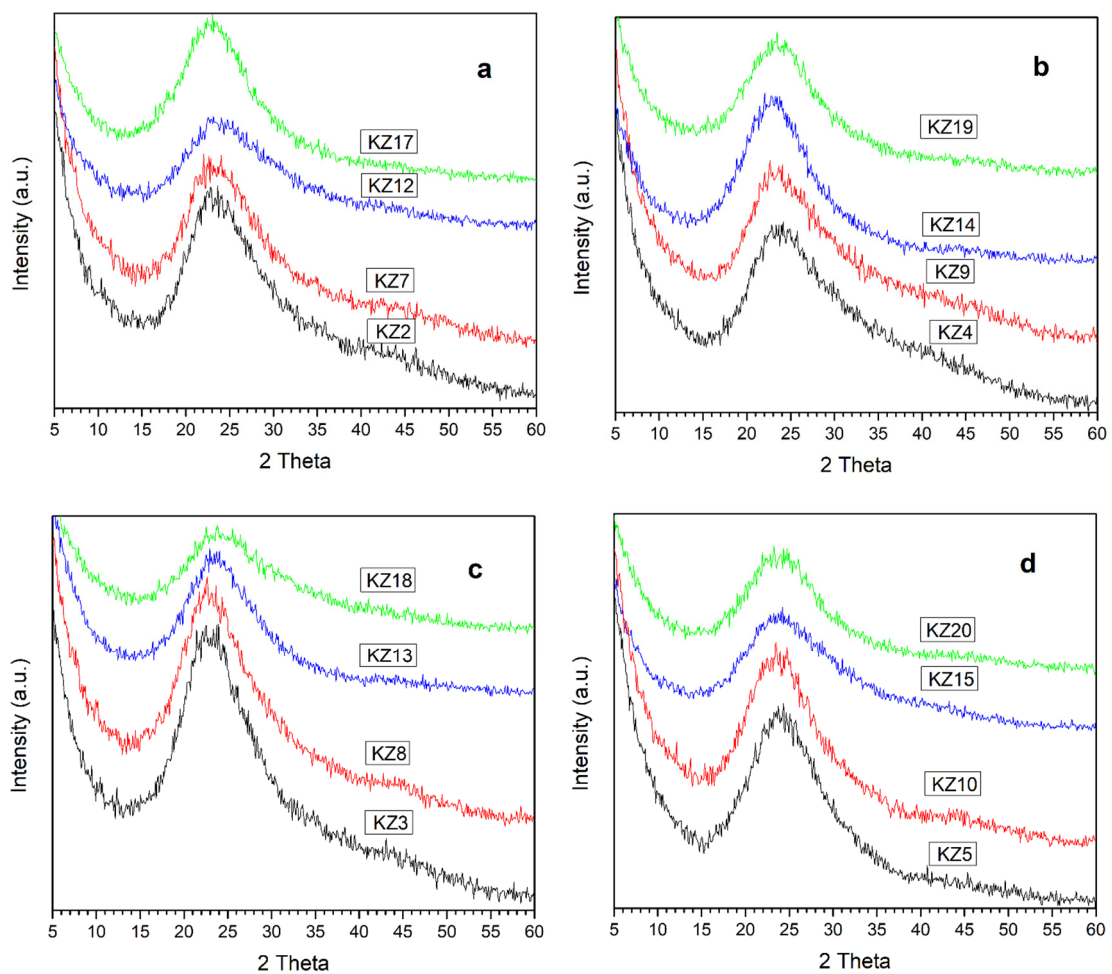


Figure 7. XRD diagram of all synthesized silica-based solids. (a) All solids synthesized with 50% orange peel. (b) All solids synthesized with 50% lemon peel. (c) All solids synthesized with 25% orange peel. (d) All solids synthesized with 25% lemon peel.

3.5. FT-IR Characterization

FT-IR spectroscopy has been widely used for the characterization of materials synthesized by the sol-gel method [51,55]. This made it possible to perform an in-depth analysis to understand the relationships between the properties of the material—including its structure at the atomic level—and the IR spectrum. As the structure evolved in the silica xerogel, a three-dimensional network of interconnected tetrahedral units formed. FT-IR allows, depending on the width and position of the bands, the characterization of the material by interpreting its composition and structure. In this study, the region of 4000–500 cm^{-1} was used.

Figure 8 shows the complete FT-IR spectrum of the samples obtained by synthesis with TEOS as a precursor and acetic acid (KZ1), citric acid (KZ6) and hydrochloric acid (KZ11) as acid catalysts and ammonium hydroxide (KZ16) as the alkaline catalyst. Table 6 shows the characteristic absorption bands of silica obtained with acetic acid as a catalyst.

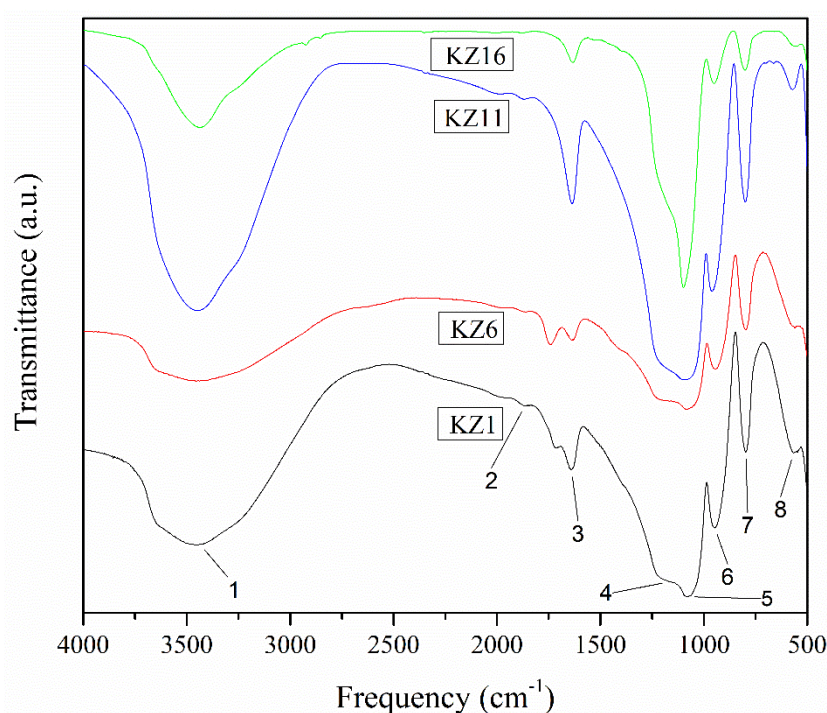


Figure 8. FT-IR spectrum of the pure silica obtained by synthesis with TEOS as a precursor and acetic acid (KZ1), citric acid (KZ6), hydrochloric acid (KZ11) and ammonium hydroxide (KZ16).

Table 6. FT-IR of silica synthesized with acetic acid (KZ1).

Bands	Wavenumber (cm^{-1})	Band Assignment	Functional Group
1	3437	ν OH ¹	O-H bonded
2	1864	$\nu\beta$ (Si-O) ²	Si-OH
3	1639	δ H-O-H ³	H-O-H
4	1166	ν S (Si-O-Si) ⁴	Si-O-Si
5	1079	ν a (Si-O-Si) ⁵	Si-O-Si
6	948	$\nu\beta$ (Si-O) ²	Si-OH
7	797	ν s (Si-O) ⁶	Si-O-Si
8	566	ν (Si-O) ¹	SiO ₂

¹ ν : vibration stretching; ² $\nu\beta$: symmetric vibration stretching; ³ δ : deformation vibration; ⁴ ν S: symmetric deformation vibration; ⁵ ν a: anti-symmetrical vibration stretching; ⁶ ν s: symmetrical vibration.

Figure 8 and Table 6 show bands at 500, 800, 950, 1080 and 1200 cm^{-1} (the five last bands), which are characteristic bands of silica, corresponding to vibrations of silicon-oxygen bonds. These bands can be classified by the movement (to roll, bend and stretch) of the oxygen atom related to the silicon atoms [56]. The symmetric and asymmetric stretching modes of the Si-O-Si bonds can be assigned to bands at 1166 and 1079 cm^{-1} , respectively. The vibration at 797 cm^{-1} is associated with the symmetric stretching of the Si-O bond or vibrational modes of structure rings. The bands centered at 948 and 1864 cm^{-1} were assigned to the vibration of the Si-O bonds (silanols) and are characteristic of silica xerogel [57]. The band located around 566 cm^{-1} was attributed to the deformation of cyclotetrasiloxanes (four-membered siloxane rings). This molecule can constitute a large fraction of the oligomeric species present in TEOS-derived systems because they are stable during the hydrolysis processes [58].

The broad band located at 3000 to 3700 cm^{-1} was assigned to the OH species due to stretching vibrations of hydrogen-bonded water molecules on the surface of silica [59], to silanols bound to molecular water and to free silanols on the surface of the gel [60,61]. The band located at 1639 cm^{-1} was assigned to the deformation of molecular water and resulted from the angular deformations of H-O-H bonds in H_2O . The description made for the KZ1 silica sample is common for the other three pure silica forms (KZ6, KZ11 and KZ16).

Figure 9 shows the FT-IR spectra of the silica-based materials obtained with 50% and 25% orange and lemon peels with acid and alkaline hydrolysis. As previously mentioned, changes in the position and shape of the absorption bands can be related to structural changes, which can occur with different solvent compositions (such as water and ethanol), leading to a variation in the hydrolysis and condensation reactions.

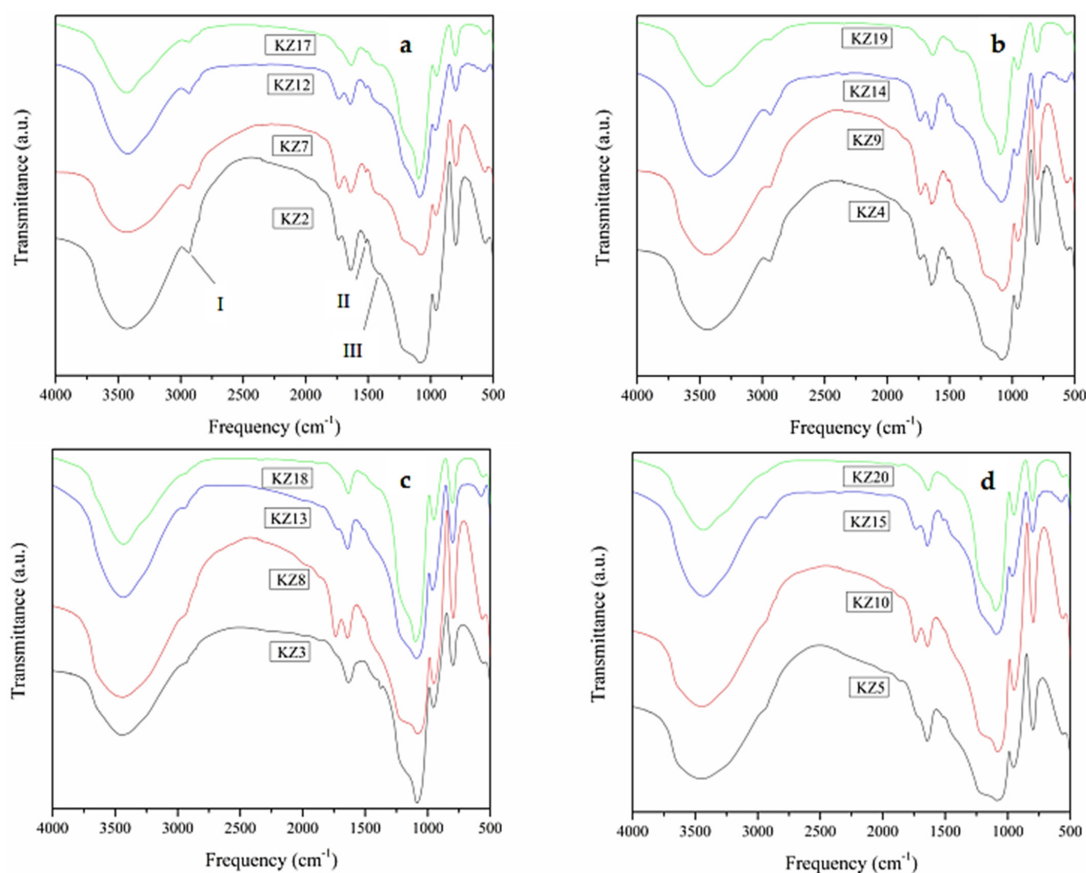


Figure 9. FT-IR spectrum of the synthesized silica. (a) All silica synthesized with 50% orange peel. (b) All silica synthesized with 50% lemon peel. (c) All silica synthesized with 25% orange peel. (d) All silica synthesized with 25% lemon peel.

For Figure 9a, the band appearing at 2932 cm^{-1} (marked as I) can be assigned to the symmetric and asymmetric stretching of the C-H bonds in the residual groups $\text{CH}_3\text{-OH}$ and $\text{CH}_3\text{-O-Si}$ [60]. In this same figure, two absorption bands are observed at 1409 and 1518 cm^{-1} (marked as II and III, respectively) due to the CH_3 groups provided by the organic material (bio-waste); these bands are characteristic of a hydrophobic form of silica. The description made for the KZ2 sample is common for the other silica-based solids synthesized with 50% and 25% orange and lemon peels.

All the characterizations used and discussed above portray the first part of a broad study, in which we highlight the initial stage of understanding the morphology and behavior of silica supports synthesized using different amounts of bio-waste and acidic and basic catalysts in order to analyze the influence that such bio-residues have on the reaction to obtain the silica-based solid support. Based on this knowledge, and also based on previous studies on the same topic [24,25], orange and lemon bio-waste can provide acidity for the reaction with the precursor TEOS. There is an indication that it would be possible to partially replace the acid catalysts used in this synthesis by bio-waste, but not completely, as they subtly reduce the acidity of the mixed materials when compared to pure silica—since the acidity of the acids used is greater than the amount of acidic compounds that are extracted from the citrus peels in the mixed matrices.

4. Conclusions

In this study, we synthesized new materials using the sol-gel method, a simple and fast technique that allowed the inclusion of bio-waste into silica matrices, proposing a first stage for the development of new silica-based supports that can be used in heterogeneous catalysis. The analyses of the influence of the orange and lemon peel percentages in the acidity and morphology of siliceous solids revealed promising results, suggesting that the bio-waste used can provide acidity to partially replace the acid catalysts investigated in acid hydrolysis—since the values obtained using 25 and 50% of bio-waste are similar to those of pure silica—but it is not possible to replace them completely. In addition, the mixed materials also showed the ability to maintain the siliceous structure. This is an important step for future studies in order to replace, for example, strong inorganic acids with a renewable raw material (bio-waste), which has a lower cost and suitable morphology. Research based on sustainability aspects is increasingly important and necessary in the current model of production and consumption in which we live. The chemistry required for a circular model will materialize only through a new attitude toward research, chemical engineering and the design of new processes and products.

Author Contributions: Conceptualization, P.G.V. and V.G.Z.; conduct of the experiments and characterization techniques, K.Z., K.I. and M.B.C.M.; prepared and wrote the draft of the manuscript, P.G.V.; supervision and editing of the final version, P.G.V. All authors have read and agreed to the published version of the manuscript.

Funding: This research received no external funding.

Institutional Review Board Statement: Not applicable.

Informed Consent Statement: Not applicable.

Data Availability Statement: More data can be obtained by request to the authors.

Acknowledgments: The authors would like to thank UNLP, CONICET, AUGM, CNPq and Capes for the financial support, at the service of FT-IR of CINDECA, Dra. R. Arreche, Dra. V. Palermo, Tco Qco L. Osiglio and G. Kürten for their collaboration in this study.

Conflicts of Interest: The authors declare no conflict of interest.

References

1. Kümmerer, K. Sustainable Chemistry: A Future Guiding Principle. *Angew. Chem. Int. Ed.* **2017**, *56*, 16420–16421. [[CrossRef](#)]
2. Kümmerer, K.; Clark, J.H.; Zuin, V.G. Rethinking Chemistry for a Circular Economy. *Science* **2020**, *367*, 369–370. [[CrossRef](#)]

3. Zuin, V.G. Circularity in Green Chemical Products, Processes and Services: Innovative Routes Based on Integrated Eco-Design and Solution Systems. *Curr. Opin. Green Sustain. Chem.* **2016**, *2*, 40–44. [[CrossRef](#)]
4. Hamilton-Smith, E. Terrestrial Ecoregions of the Indo-Pacific: A Conservation Assessment. *Electron. Green J.* **2002**, *1*. [[CrossRef](#)]
5. Satari, B.; Karimi, K. Citrus Processing Wastes: Environmental Impacts, Recent Advances, and Future Perspectives in Total Valorization. *Resour. Conserv. Recycl.* **2018**, *129*, 153–167. [[CrossRef](#)]
6. García, R.M.L. La agricultura ecológica en el quehacer científico. Tema incipiente en la geografía. *An. Geogr. Univ. Complut.* **1999**, *19*, 351.
7. DeLind, L.B. Transforming Organic Agriculture into Industrial Organic Products: Reconsidering National Organic Standards. *Hum. Organ.* **2000**, *59*, 198–208. [[CrossRef](#)]
8. Planella, J.; Pagès Santacana, A.; Darnell i Vianya, M. *Antropologia de l'Educació*; Editorial UOC: Barcelona, Spain, 2007; ISBN 978-84-9788-576-8.
9. Willer, E.H.; Lernoud, J. *The World of Organic Agriculture-Statistics and Emerging Trends 2019*; Research Institute of Organic Agriculture (FiBL) and IFOAM—Organics International: Frick, Switzerland, 2019; 356p.
10. Willer, E.H.; Schlatter, B.; Trávní, J.; Kemper, L.; Lernoud, J. *The World of Organic Agriculture Statistics and Emerging Trends 2020*; Research Institute of Organic Agriculture (FiBL) and IFOAM—Organics International: Frick, Switzerland, 2020; 337p.
11. Paull, J.; Hennig, B. Atlas of Organics: Four Maps of the World of Organic Agriculture. *J. Org.* **2016**, *3*, 25–32.
12. Sarris, A. *Medium-Term Prospects for Agricultural Commodities: Projections to the Year 2010*; Food and Agriculture Organization of the United Nations, Ed.; Food and Agriculture Organization of the United Nations: Rome, Italy, 2003; ISBN 978-92-5-105077-4.
13. Sharma, K.; Mahato, N.; Cho, M.H.; Lee, Y.R. Converting Citrus Wastes into Value-Added Products: Economic and Environmentally Friendly Approaches. *Nutrition* **2017**, *34*, 29–46. [[CrossRef](#)]
14. Ananthi, A.; Ramesh, D. Preparation and Characterization of Silica Material from Rice Husk Ash-An Economically Viable Method. *Chem. Mater. Res.* **2016**, *8*, 1–7.
15. Shreya, M.K.; Indhumathi, C.; Rajarajeswari, G.R.; Ashokkumar, V.; Preethi, T. Facile Green Route Sol–Gel Synthesis of Nano-Titania Using Bio-Waste Materials as Templates. *Clean Technol. Environ. Policy* **2021**, *23*, 163–171. [[CrossRef](#)]
16. Boffa, V.; Perrone, D.G.; Magnacca, G.; Montoneri, E. Role of a Waste-Derived Polymeric Biosurfactant in the Sol–Gel Synthesis of Nanocrystalline Titanium Dioxide. *Ceram. Int.* **2014**, *40*, 12161–12169. [[CrossRef](#)]
17. Patel, K.G.; Shettigar, R.R.; Misra, N.M. Recent Advance in Silica Production Technologies from Agricultural Waste Stream–Review. *J. Adv. Agric. Technol.* **2017**, *4*, 274–279. [[CrossRef](#)]
18. Srinath, P.; Azeem, P.A.; Reddy, K.V. Sol-Gel Synthesis of SiO₂-CaO-Na₂O Bio-Ceramics Using Bio-Waste. *AIP Conf. Proc.* **2020**, *2265*, 030042.
19. Silvestri, B.; Vitiello, G.; Luciani, G.; Calcagno, V.; Costantini, A.; Gallo, M.; Parisi, S.; Paladino, S.; Iacomino, M.; D'Errico, G.; et al. Probing the Eumelanin–Silica Interface in Chemically Engineered Bulk Hybrid Nanoparticles for Targeted Subcellular Antioxidant Protection. *ACS Appl. Mater. Interfaces* **2017**, *9*, 37615–37622. [[CrossRef](#)]
20. Gonzalo-Juan, I.; Riedel, R. Ceramic Synthesis from Condensed Phases. *Chem. Texts* **2016**, *2*, 6. [[CrossRef](#)]
21. Igal, K.; Vázquez, P. Antimicrobial Fabrics Impregnated with Ag Particles Included in Silica Matrices. In *Waste in Textile and Leather Sectors*; Körlü, A., Ed.; IntechOpen: London, UK, 2020; ISBN 978-1-78985-243-1.
22. Igal, K.; Arreche, R.A.; Sambeth, J.E.; Bellotti, N.; Vega-Baudrit, J.R.; Redondo-Gómez, C.; Vázquez, P.G. Antifungal Activity of Cotton Fabrics Finished Modified Silica-Silver-Carbon-Based Hybrid Nanoparticles. *Text. Res. J.* **2019**, *89*, 825–833. [[CrossRef](#)]
23. Pota, G.; Venezia, V.; Vitiello, G.; Di Donato, P.; Mollo, V.; Costantini, A.; Avossa, J.; Nuzzo, A.; Piccolo, A.; Silvestri, B.; et al. Tuning Functional Behavior of Humic Acids through Interactions with Stöber Silica Nanoparticles. *Polymers* **2020**, *12*, 982. [[CrossRef](#)]
24. Migliorero, M.B.C.; Palermo, V.; Vázquez, P.G.; Romanelli, G.P. Valorization of Citrus Waste: Use in Catalysis for the Oxidation of Sulfides. *J. Renew. Mater.* **2017**, *5*, 167–173. [[CrossRef](#)]
25. Palermo, V.; Igal, K.; Colombo Migliorero, M.B.; Sathicq, A.G.; Quaranta, N.; Vazquez, P.G.; Romanelli, G.P. Valorization of Different Wastes and Their Use for the Design of Multifunctional Eco-Catalysts. *Waste Biomass Valorization* **2017**, *8*, 69–83. [[CrossRef](#)]
26. Yilmaz, E.; Soylak, M. Functionalized Nanomaterials for Sample Preparation Methods. In *Handbook of Nanomaterials in Analytical Chemistry*; Elsevier: Amsterdam, The Netherlands, 2020; pp. 375–413. ISBN 978-0-12-816699-4.
27. Zanella, R. Metodologías Para La Síntesis de Nanopartículas Controlando Forma y Tamaño. *Mundo Nano Rev. Interdiscip. En Nanociencia Nanotecnol.* **2014**, *5*, 69–81. [[CrossRef](#)]
28. Brinker, C.J.; Scherer, G.W. *Sol.-Gel Science: The Physics and Chemistry of Sol.-Gel Processing*; Academic Press, INC: San Diego, CA, USA, 2013; ISBN 978-0-08-057103-4.
29. Fidalgo, A.; Ilharco, L.M. Correlation between Physical Properties and Structure of Silica Xerogels. *J. Non-Cryst. Solids* **2004**, *347*, 128–137. [[CrossRef](#)]
30. Jiménez-González, C.; Curzons, A.D.; Constable, D.J.C.; Cunningham, V.L. Expanding GSK's Solvent Selection Guide? Application of Life Cycle Assessment to Enhance Solvent Selections. *Clean Technol. Environ. Policy* **2004**, *7*, 42–50. [[CrossRef](#)]
31. Cordero Castaño, A.F. Nuevos Materiales Utilizados Para la Obtención de Ecocatalizadores a Partir de Bio-Residuos. Ph.D. Thesis, Universidad Nacional de La Plata, La Plata, Argentina, 2020.
32. Schmidt, H. New Type of Non-Crystalline Solids between Inorganic and Organic Materials. *J. Non-Cryst. Solids* **1985**, *73*, 681–691. [[CrossRef](#)]

33. Mendoza, E.; García, C. Recubrimientos por Sol-Gel Sobre Sustratos de Acero Inoxidable, Revisión del Estado del Arte. *Dyna* **2007**, *74*, 101–110.
34. Matlack, A.S. *Introduction to Green Chemistry*, 2nd ed.; CRC Press: Boca Raton, FL, USA, 2010; ISBN 978-1-4200-7811-4.
35. Byrne, F.P.; Jin, S.; Paggiola, G.; Petchey, T.H.M.; Clark, J.H.; Farmer, T.J.; Hunt, A.J.; Robert McElroy, C.; Sherwood, J. Tools and Techniques for Solvent Selection: Green Solvent Selection Guides. *Sustain. Chem. Process.* **2016**, *4*, 7. [[CrossRef](#)]
36. Milea, C.A.; Bogatu, C.; Du, A. The Influence of Parameters in Silica Sol-Gel Process. *Bull. Transilv. Univ. Brasov. Eng. Sci. Ser. I* **2011**, *4*, 59.
37. Arreche, R. Inclusión de Ag en Materiales Basados en Sílice y Circonia, Sintetizados Por el Método Sol-Gel, Para Su aplicación Como Aditivos Antimicrobianos en Pinturas. Ph.D. Thesis, Universidad Nacional de La Plata, La Plata, Argentina, 2016.
38. Igal, K. Telas Antimicrobianas Impregnadas Con Partículas de Ag o Zn Reciclado Incluidas en Matrices Silíceas Modificadas. Ph.D. Thesis, Universidad Nacional de La Plata, La Plata, Argentina, 2019.
39. Meixner, D.L.; Dyer, P.N. Influence of Sol-Gel Synthesis Parameters on the Microstructure of Particulate Silica Xerogels. *J. Sol.-Gel Sci. Technol.* **1999**, *14*, 223–232. [[CrossRef](#)]
40. de Gennes, P.-G. *Scaling Concepts in Polymer Physics*; Cornell University Press: New York, NY, USA, 1979; ISBN 978-0-8014-1203-5.
41. Kirkbir, F.; Murata, H.; Meyers, D.; Chaudhuri, S.R.; Sarkar, A. Drying and Sintering of Sol-Gel Derived Large SiO₂ Monoliths. *J. Sol.-Gel Sci. Technol.* **1996**, *6*, 203–217. [[CrossRef](#)]
42. Soleimani Dorcheh, A.; Abbasi, M.H. Silica Aerogel; Synthesis, Properties and Characterization. *J. Mater. Process. Technol.* **2008**, *199*, 10–26. [[CrossRef](#)]
43. Carman, P.C. Constitution of Colloidal Silica. *Trans. Faraday Soc.* **1940**, *36*, 964–973. [[CrossRef](#)]
44. Romanelli, G.; Vázquez, P.; Pizzio, L.; Quaranta, N.; Autino, J.; Blanco, M.; Cáceres, C. Phenol Tetrahydropyranylation Catalyzed by Silica-Alumina Supported Heteropolyacids with Keggin Structure. *Appl. Catal. Gen.* **2004**, *261*, 163–170. [[CrossRef](#)]
45. Curran, M.D.; Stiegman, A.E. Morphology and Pore Structure of Silica Xerogels Made at Low PH. *J. Non-Cryst. Solids* **1999**, *249*, 62–68. [[CrossRef](#)]
46. Zhao, S.; Xu, D.; Ma, H.; Sun, Z.; Guan, J. Controllable Preparation and Formation Mechanism of Monodispersed Silica Particles with Binary Sizes. *J. Colloid. Interface Sci.* **2012**, *388*, 40–46. [[CrossRef](#)] [[PubMed](#)]
47. Tadanaga, K.; Morita, K.; Mori, K.; Tatsumisago, M. Synthesis of Monodispersed Silica Nanoparticles with High Concentration by the Stöber Process. *J. Sol.-Gel Sci. Technol.* **2013**, *68*, 341–345. [[CrossRef](#)]
48. Zarib, N.S.M.; Abdullah, S. Effect of C₆H₈O₇ Concentration on Silica Extraction of Rice Husk, Rice Husk Ash and Mixture of Rice Husk With Rice Husk Ash Via Acid Leaching Process. *Int. J. Eng.* **2018**, *7*, 190–195.
49. Saini, J.; Garg, V.K.; Gupta, R.K. Green Synthesized SiO₂@OPW Nanocomposites for Enhanced Lead (II) Removal from Water. *Arab. J. Chem.* **2020**, *13*, 2496–2507. [[CrossRef](#)]
50. Cui, J.; Sun, H.; Luo, Z.; Sun, J.; Wen, Z. Preparation of Low Surface Area SiO₂ Microsphere from Wheat Husk Ash with a Facile Precipitation Process. *Mater. Lett.* **2015**, *156*, 42–45. [[CrossRef](#)]
51. Worathanakul, P.; Trisuwan, D.; Phatrak, A.; Kongkachuichay, P. Effect of Sol-Gel Synthesis Parameters and Cu Loading on the Physicochemical Properties of a New SUZ-4 Zeolite. *Colloids Surf. Physicochem. Eng. Asp.* **2011**, *377*, 187–194. [[CrossRef](#)]
52. Czarnobaj, K. Preparation and Characterization of Silica Xerogels as Carriers for Drugs. *Drug Deliv.* **2008**, *15*, 485–492. [[CrossRef](#)]
53. Ng, E.-P.; Mohammad, A.G.S.; Rigolet, S.; Daou, T.J.; Mintova, S.; Ling, T.C. Micro-and Macroscopic Observations of the Nucleation Process and Crystal Growth of Nanosized Cs-Pollucite in an Organotemplate-Free Hydrosol. *New J. Chem.* **2019**, *43*, 17433–17440. [[CrossRef](#)]
54. Pakizeh, M.; Omidkhan, M.R.; Zarringhalam, A. Synthesis and Characterization of New Silica Membranes Using Template-Sol-Gel Technology. *Int. J. Hydrogen Energy* **2007**, *32*, 1825–1836. [[CrossRef](#)]
55. Hu, S.; Hsieh, Y.-L. Preparation of Activated Carbon and Silica Particles from Rice Straw. *ACS Sustain. Chem. Eng.* **2014**, *2*, 726–734. [[CrossRef](#)]
56. Kirk, C.T. Quantitative Analysis of the Effect of Disorder-Induced Mode Coupling on Infrared Absorption in Silica. *Phys. Rev. B* **1988**, *38*, 1255–1273. [[CrossRef](#)] [[PubMed](#)]
57. Wong, S.-F.; Deekomwong, K.; Wittayakun, J.; Ling, T.C.; Muraza, O.; Adam, F.; Ng, E.-P. Crystal Growth Study of K-F Nanozeolite and Its Catalytic Behavior in Aldol Condensation of Benzaldehyde and Heptanal Enhanced by Microwave Heating. *Mater. Chem. Phys.* **2017**, *196*, 295–301. [[CrossRef](#)]
58. Araujo-Andrade, C.; Ortega-Zarzosa, G.; Selina, P.; Martinez, J.R.; Villegas-Aguirre, F.; Ruiz, F. Análisis de Las Reacciones de Hidrólisis y Condensación En Muestras de Sílica Xerogeles Usando Espectroscopía Infrarroja. *Rev. Mex. Fis.* **2000**, *46*, 593–597.
59. Orcel, G.; Phalippou, J.; Hench, L.L. Structural Changes of Silica Xerogels during Low Temperature Dehydration. *J. Non-Cryst. Solids* **1986**, *88*, 114–130. [[CrossRef](#)]
60. Martinez, J.R.; Ruiz, F. Mapeo estructural de sílica xerogel utilizando espectroscopía infrarroja. *Rev. Mex. Fis.* **2002**, *48*, 142–149.
61. Duran, A.; Serna, C.; Fornes, V.; Fernandez Navarro, J.M. Structural Considerations about SiO₂ Glasses Prepared by Sol-Gel. *J. Non-Cryst. Solids* **1986**, *82*, 69–77. [[CrossRef](#)]